Comparison of Dynamic Characteristics of Virtual Synchronous Machine Control Algorithms

T. THILEKHA[1], S. FILIZADEH[1], U. ANNAKKAGE[1], C. KARAWITA[2]
[1]University of Manitoba
[2]TransGrid Solutions (Pvt.) ltd.
Canada

SUMMARY

Proliferation of distributed generators (DG) such as solar and wind power plants have caused a paradigm shift in generation from large-scale, localized synchronous machines (SMs) to small-scale, dispersed, inverter-tied resources. With this shift, important underpinnings of a power system experience radical changes. The inertia of a power system indicates its robustness in absorbing generation-load imbalances in order to maintain the grid frequency and voltage at their nominal conditions. The large rotating masses of SM rotors have inertia and help in maintaining system stability. Due to the absence of rotational masses in inverter-interfaced DG schemes, the system inertia is drastically reduced, which leads to poor recovery from a fault and large frequency swings subsequent to disturbances.

Alternative methods for control of DG inverters are being explored in which they are operated to emulate the behaviour of a synchronous machine with inertial characteristics. These virtual synchronous machine (VSM) methods use specialized algorithms to give a voltage source converter (VSC) the characteristic features of a synchronous machine with arbitrary parameters such as damping and inertia. Several VSM algorithms are proposed in the literature that may or may not rely on a phase-locked loop (PLL), including VSM zero-inertia (VSM0H), voltage controlled-VSC (VC-VSC) model, synchronverters, and modified VSM0H method. Except the VSM0H algorithm all the other algorithms can emulate inertia. These algorithms provide greatly different opportunities for emulation of inertia and need to be fully investigated and assessed in order to enable their judicious adoption.

This paper presents a detailed comparative study of the aforementioned VSM algorithms using extensive electromagnetic transient (EMT) simulations of an inverter with different VSM algorithms connected to a load. The ability of each VSM algorithm is assessed in terms of its dynamic response and performance in supporting the grid's frequency and voltage in response to load variations and faults. The contributions of this paper are essential to establish the true merits of VSM algorithms and will be of immediate use to practicing engineers who need to implement such algorithms for inverter controls.

KEYWORDS

Virtual synchronous machines (VSM), inertia, damping, frequency droop, voltage droop, transient response, steady state response.

muthukut@myumanitoba.ca

1. INTRODUCTION

With the proliferation of renewable energy sources, a paradigm shift from large-scale, concentrated power generation to small-scale, distributed generation has occurred [1]. As a result, inadequate inertia and lower damping of power system transients are more prevalent than before [2], [3]. To combat diminishing inertia, methods that deploy power-electronic converters are explored. A converter controlled in a way to emulate the characteristics of a synchronous machine (SM) is called a virtual synchronous machine (VSM). VSM implementation comprises a mathematical model of a SM, and presently there are a number of VSM algorithms [4]. The parameters of a VSM may be selected - without significant constraint - to emulate an arbitrary SM [4]. VSM applications are varied, including smooth transition between grid-connected and islanded operation in micro-grids, battery charging applications to support grid frequency, and grid support in HVDC transmission schemes [5], to name a few. In this paper, four VSM algorithms are assessed to identify their dynamic response characteristics. The studies reported in the paper are conducted using detailed simulations in PSCAD/EMTDC. The results clearly show the impact of the inertia emulation loop on the frequency nadir. The impact of the controller topology on the fault current level has also been observed.

2. THE ANALOGY BETWEEN A SM AND A VSM

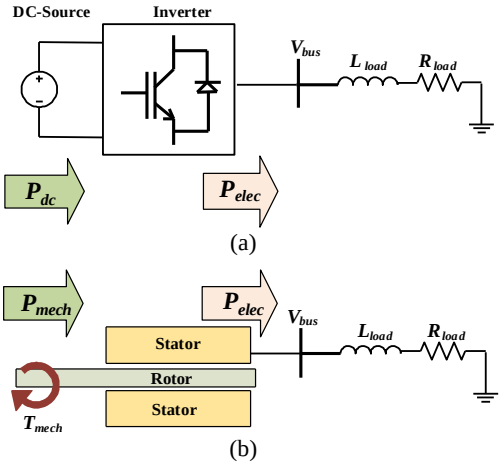

Figure 1. The comparison of (a) a VSM connected to load. (b) a SM connected to load

An interpretation of the physics of an electromechanical SM can be implemented with a power electronic converter controlled by a VSM algorithm (Figure 1). A VSM mimics the dynamic behaviour of a SM, provided that it has an adequately large and readily accessible dc-side system to support its active power exchanges with the ac grid. VSM algorithm built on the swing equation with frequency droop and a separate reactive power-voltage controller are considered in this paper.

The mechanical power given to a SM through its rotor is analogous to the dc power given to a converter. In steady state, the electrical power output of a SM is equal to its mechanical power input. Similarly, the electrical power output from a converter is equal to the dc power input at steady state. A new steady-state operating point for a SM is established by controlling the mechanical power according to the frequency droop by adjusting the prime mover settings. A VSM modulates its dc power by changing the duty ratios of its switches to reach a new steady state operating point. The response of a SM without its governor action is determined by its inertia and damping constant [6]. The transient response of a SM, which forms the basis of most VSM algorithms, is described by the classical swing equation shown in (1).

$$P_{mech} - P_{elec} = 2H\left(\frac{d^2\delta}{dt^2}\right) + K_D\left(\frac{d\delta}{dt}\right) \quad (1)$$

Where P_{mech}, P_{elec}, K_D, H, and δ are the mechanical input power, electrical output power, damping coefficient, inertia time-constant, and angular position of the rotor in electrical radians, respectively. The energy stored in the rotating mass of a SM's rotor is the primary source/sink for absorbing power imbalances. A VSM algorithms built on the swing equation can emulate the inertia, and the energy required to fulfill its energy exchanges with the grid need to be provided from the converter's dc-side system, which may include an energy storage system (ESS) with fast acting capability and high-power density. Capacitors, super-capacitors, batteries, and flywheels are possible candidates for inertia emulation [7].

The damping torque is created in SM according to the Faraday's Law. The deviation in speed followed by a disturbance creates a flux component in the damper windings, which in return creates an induced

EMF and a current. The flux generated due to this current creates a torque that counteracts the main torque and has a damping effect on the oscillations [8]. The power losses in the damper winding also need to be supplied by an energy source accessible to the VSM. Eventually, the droop controller changes the power generation of SM at the expense of a frequency deviation from the original value. To emulate the droop action, a VSM requires a slow acting ESS with high energy capacity. Batteries are suitable candidates for droop action emulation. In the VSM models considered here the secondary frequency control action that restores the frequency is not included.

3. OVERVIEW OF VSM ALGORITHMS

The grid-forming capability of the selected VSM algorithms is tested using a system (Figure 2) consisting of a two-level converter connected to load via an LCL filter, a step-up transformer, and a short transmission line of 10 km. The system is modelled in PSCAD/EMTDC. The LCL filter is tuned to reduce the current harmonics below 5% (according to IEEE1547 standard). All controllers are per unitized. Test system specifications are given in Table 1. Table 2 shows the transmission line parameters. The respective parameters of the control algorithms are set to be equal for a fair comparison of the algorithms.

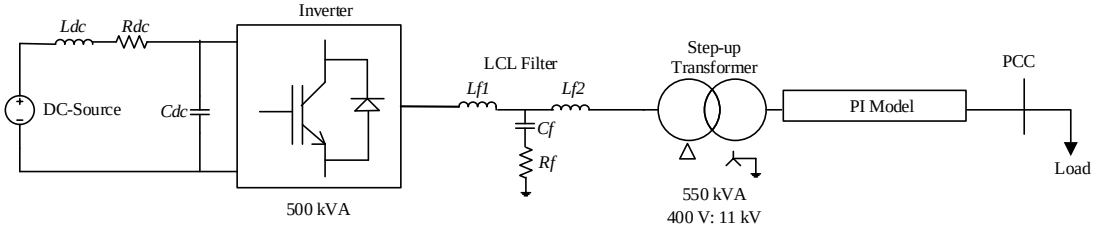

Figure 2. The single line diagram of the test system

Table 1. Parameters of the test system

Parameter	Value	Parameter	Value
dc voltage	4 kV	L_{f1}	150 μH
R_{dc}	0.0006 Ω	L_{f2}	5 μH
L_{dc}	0.1 H	C_f	828.93 μF
C_{dc}	312.5 μF	R_f	0.08 Ω
Converter rating	500 kVA	Transformer leakage reactance	0.1 pu
Switching Frequency	2 kHz	Transformer copper loss	0.01 pu
Fixed P-component of load	0.6 pu	Step P-component of load	0.1 pu
Fixed Q-component of load	0.6 pu	Step Q-component of load	0.1 pu

Table 2. Parameters of the short transmission line

	$R1(\Omega/km)$	$X1(\Omega/km)$	$Y1(\mu s/km)$	$R0(\Omega/km)$	$X0(\Omega/km)$	$Y0(\mu s/km)$
Value	0.103	0.405	4.117	0.279	1.902	0

3.1. Virtual Synchronous Machine Zero Inertia (VSM0H) Model

VSMOH model uses only the conventional droop control equations to attain the target frequency and voltage, so that the converter can be controlled as a voltage source. Though the VSM0H model incompetents inertia support, the droop action responds to frequency deviation [9]. Further this control strategy makes the converter to source or sink unbalanced harmonics and inter-harmonic currents, which helps to maintain the point of common coupling (PCC) voltage and power quality. The VSM0H model does not require a PLL. Though the original controller includes a filter for adding further damping, this piece of work has ignored this, on the basis of insignificant added advantage. A boxcar filter (moving average filter) has been used in the previous work to filter the instantaneous power values. This acts as a low-pass filter with zeros at every integer multiple frequency of 1/*T*, where *T* is the window size. This work uses a low-pass filter with a bandwidth of 60 Hz, which removes the higher order harmonics and produces a much simpler controller structure. Due to the absence of the swing equation, the response is fast compared to other VSM algorithms based on the swing equation. The controller composition is given in Figure 3.

The only required measurement is the current flowing from the converter. The target frequency (f_{set}), the target voltage (v_{set}), the set active power command (P_{set}), the set reactive power command (Q_{set}), frequency droop (D_f) and voltage droop (D_v) should be supplied externally. Inbuilt droop action facilitates parallel operation of VSM0H controlled converters. The parameters are set as, P_{set}= Q_{set} =

0.6 pu, f_{set}=1 pu, v_{set}=1.2 pu, f_{set}= 50 Hz, D_f = 0.03 pu, D_v= 0.03 pu. The response of the VSM0H to large signal disturbances is discussed in the next section.

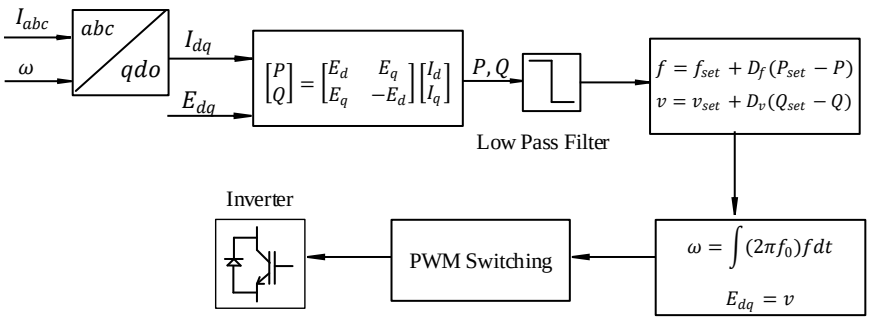

Figure 3. The VSM0H control algorithm

3.1.1. VSM0H time-domain simulation results

A constant-power resistive load of 0.1 pu and a constant-impedance inductive load of 0.1 pu are added to obtain the responses in Figures 4 and 5, respectively. The 0.1 pu constant-power resistive load increases the active power demand by 0.1 pu (Figure 4.a). Due to the coupling between active and reactive power, reactive power supply also undergoes transients (Figure 4.b). The unavailability of a secondary frequency control action results in a speed deviation at the steady state. The steady state speed value is determined by the *f*-droop action. Since $\Delta f/\Delta P = D_f$, For a ΔP = 0.1 pu and D_f = 0.03 pu, Δf is 0.003 pu. The simulated results verify this (Figure 4.c). The external frequency measurement taken from PLL has high frequency noise due to the converter's switching action (Figure 4.d). The required additional active power has been taken from proper modulation of the dc side (Figure 4.e).

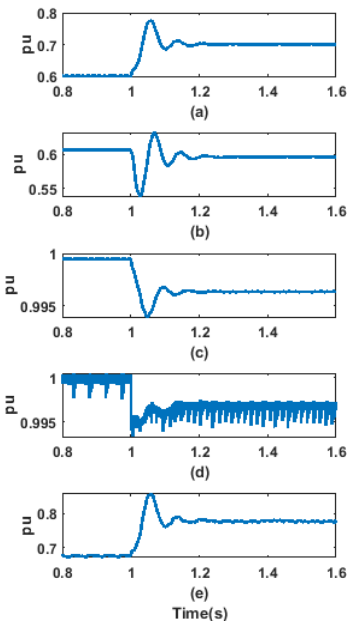

Figure 4. Constant power-resistive load of 0.1 pu addition. (a). Active power PCC (b). Reactive power PCC (c). Virtual rotor speed (d). External frequency (PLL) (e). dc power

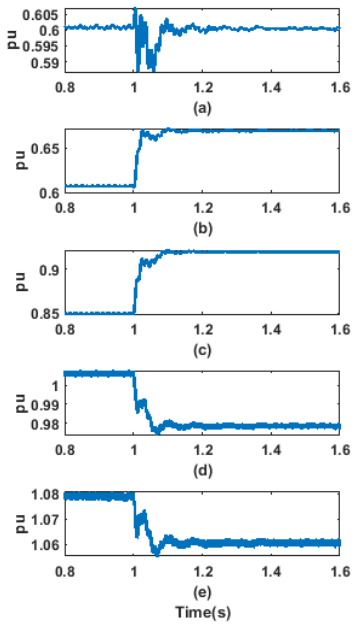

Figure 5. Constant impedance-inductive load of 0.1 pu addition. (a). Active power PCC (b). Reactive power PCC (c). Load current (d). Bus voltage (e). Machine terminal voltage

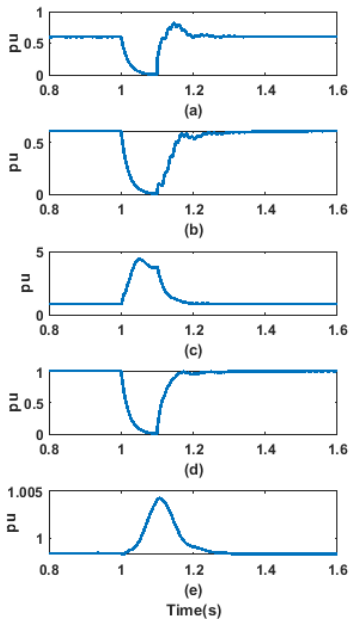

Figure 6. Three phases to ground solid fault at PCC for 0.1 s. (a). Active power PCC (b). Reactive power PCC (c). Load current (d). Bus voltage (e). Virtual rotor speed

Due to the constant-impedance nature of the inductive load, the additional reactive power supply is less than 0.1 pu (Figure 5.b). The coupling effect causes transients in the active power supply (Figure 5.a). The voltage control is governed by two actions. The Q-V droop governs the VSM's terminal voltage (Figure 5.e.). The V-I characteristic depends on the reactance between the terminal of VSM and the bus, which will determine the additional voltage drop required (Figure 5.d). Both the droops will determine the reactive power support share by parallel connection of VSM0H converters. An analysis on the phase angle together with the rms value analysis on the load current (Figure 5.b) shows

that more inductive current is drawn to support the added inductive load. The impact on the dc side power is negligible. A solid three-phase-to-ground fault is applied for 0.1 s (6-cycles). As the bus voltage reaches zero (Figure 6.d) the machine's output power at the bus reaches zero (Figures 6.a and 6.b). The fault current level reaches 4.5 pu (Figure 6.c). Due to the sudden drop of power supply, the virtual rotor accelerates similar to a conventional synchronous machine.

3.2. Voltage Controlled-VSC (VC-VSC) Model

The VC-VSC model adds the swing equation to the VSM0H model to emulate synthetic inertia and damping terms (Figure 7). The droop action modulates the virtual mechanical power input. The damping path does not contribute to the grid forming mode, as the ω_{pcc} is same as the virtual machine speed. The original work contains an additional path to control reactive power under grid connected mode [10]. This path is removed here as the focus is on the islanded mode. The generated voltage (E) is used to find out the modulation index. Then the modulation index together with the virtual phase angle is used to generate the reference waveforms for the PWM switching action. The previous work has missed the Q_{ref} in the voltage droop block. This has been added in this work. The developed islanding detection and over-current limiting actions in the original work are excluded to create a fair comparison. The absence of the emulated field action avoids the restoration of the terminal voltage. This avoids the emulation of SM dynamics optimally in this model as well. Only the transient responses will be changed from the VSM0H model, due to the inner controller part based on the swing equation of the P-*f* controller. The steady state response, which will depend on the droop action, will be same for VSM0H and VC-VSC models. A PLL is also needed for frequency measurement. The reference commands should be provided externally. The inertia, damping, and droop coefficients can be selected arbitrary. The parameters are set as, $P_{\text{ref}} = Q_{\text{ref}} = 0.6$ pu, $\omega_{\text{ref}} = 1$ pu, $E_{\text{ref}} = 1.2$ pu, $D_{\text{p}} = 0.03$ pu, $D_{\text{q}} = 0.03$ pu, $H = 3$ s, $K_{\text{D}} = 20$ pu. The dynamic responses of VSM under this algorithm are discussed next.

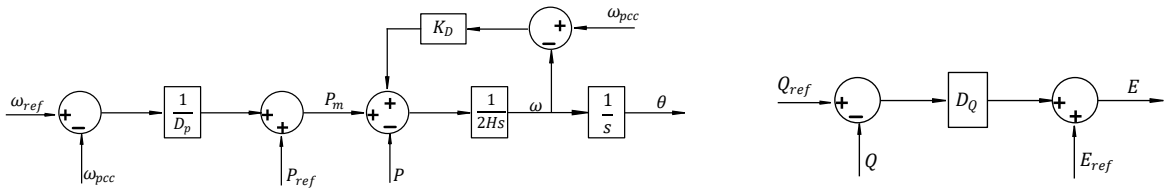

Figure 7. VC-VSC control algorithm (a) Active Power-Frequency (P-F) controller (b) Reactive Power-Voltage (Q-V) controller

3.2.1. VC-VSC model-time domain simulation results

The VC-VSC model's response to a constant-power resistive load addition is comparable to the VSMOH model (Figure 8). The transient speed variation has a sluggish behaviour due to the inbuilt swing equation model (Figure 8.c). Similar to the VSM0H model, the steady values match the *f*-droop calculations. The same Q-V controller adoption has made sure a similar response for the constant-impedance inductive load addition (Figure 9). This VSM model responds to the three-phase-to-ground solid fault at the PCC similarly to the VSM0H model (Figure 10), except the virtual rotor's peak value speed, which is 0.001 pu less than the VSM0H model (Figure 10.e). This is due to the added virtual mass for slowing down speed deviations.

3.3. Synchronverter

The synchronverter model also uses decoupled control loops for active power-frequency (P-*f*) and reactive power-voltage (Q-V) control [11], where the P-*f* controller is based on swing equation and droop action. synchronverter can emulate the field action to control the terminal voltage on top of the voltage droop action. The original synchronverter algorithm uses a mechanical damping signal to emulate frequency droop action, which results in theoretical conflicts. As mechanical damping is proportional to the speed deviation between the machine and the PCC while frequency droop action is

proportional to the speed deviation between the nominal value and the PCC frequency value. Therefore, it is worth noting that the synchronverter has eliminated the load damping path (which is actually useless in grid forming) and only frequency-droop path has used. Though the original work has used calculated torque and reactive power values for the controller design, this piece of work has only relied on the measured values. The controller arrangement is given in Figure 11.

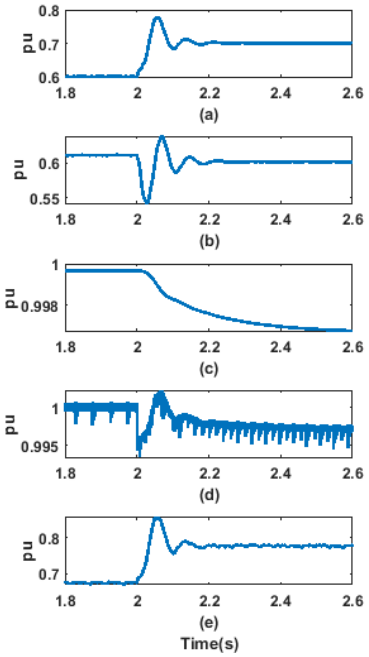

Figure 8. Constant power-resistive load of 0.1 pu addition. (a). Active power PCC (b). Reactive power PCC (c). Virtual rotor speed (d). External frequency (PLL) (e). dc power

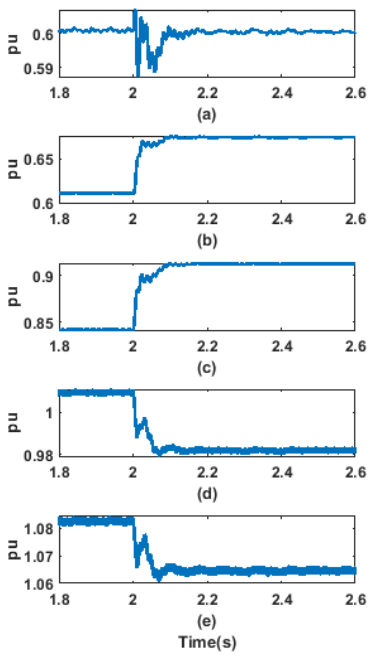

Figure 9. Constant impedance-inductive load of 0.1 pu addition. (a). Active power PCC (b). Reactive power PCC (c). Load current (d). Bus voltage (e). Machine terminal voltage

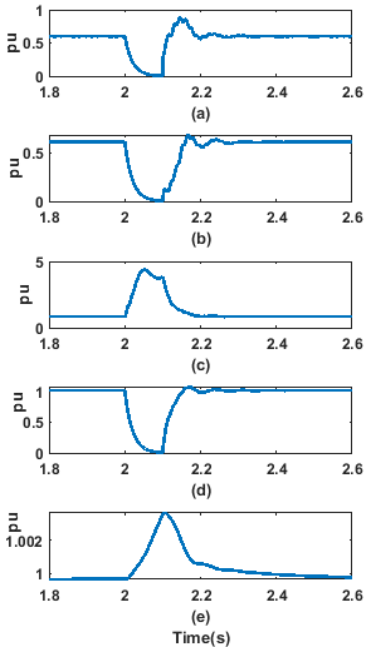

Figure 10. Three phases to ground solid fault at PCC for 0.1 s. (a). Active power PCC (b). Reactive power PCC (c). Load current (d). Bus voltage (e). Virtual rotor speed

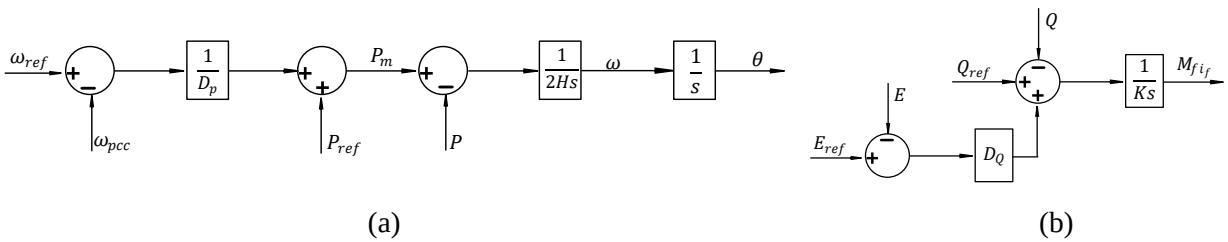

(a) (b)

Figure 11. Synchronverter control algorithm (a) Active Power-Frequency (P-F) controller (b) Reactive Power-Voltage (Q-V) controller

For a stable controller operation, the Q-V controller time constant (K) should be larger than the P-f controller time constant ($2HD_p$). The parameters are set as, $P_{ref} = Q_{ref} = 0.6$ pu, $\omega_{ref} = 1$ pu, $E_{ref} = 1.2$ pu, $D_p = 33.33$ pu, $D_q = 33.33$ pu, $H = 3$ s, $K = 3.33$ pu. The peak value of the voltage (V_m) is calculated using (2). This is then used to determine the modulation index and to generate reference signals for PWM action.

$$V_m = \omega M_f i_f \quad (2)$$

The original authors have modified the synchronverter to be self-synchronized with the grid [3]. Due to the focus on grid formation, this part is not included in this paper. However, this removal of non-linear slow acting element from the power system makes the system controlling much easier.

3.3.1. Synchronverter model time-domain simulation results

Since the P-f control path is similar to the VC-VSC model, the dynamic response of the synchronverter to a 0.1 pu addition of a constant-power load is close to that of the VC-VSC model (Figure 12). The voltage regulating action in the Q-V controller restores the machine's terminal voltage (Figure 13.e) for the constant-impedance inductive load addition. For the three-phase-to-ground solid fault, the power output, bus voltage, load current and speed deviation are closer to

previous controller algorithms. However, a slow Q-V controller has given the converter a longer a settling time than the previous two controllers.

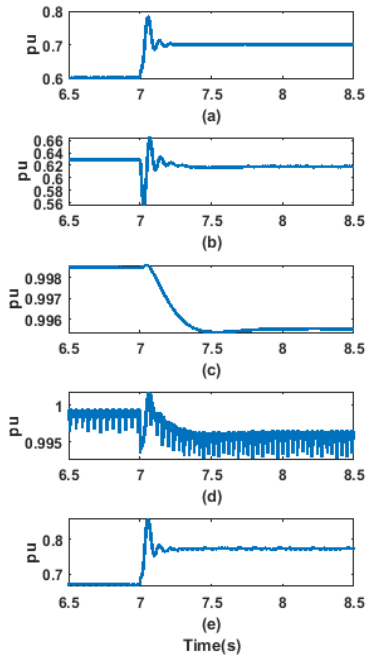

Figure 12. Constant power-resistive load of 0.1 pu addition. (a). Active power PCC (b). Reactive power PCC (c). Virtual rotor speed (d). External frequency (PLL) (e). dc power

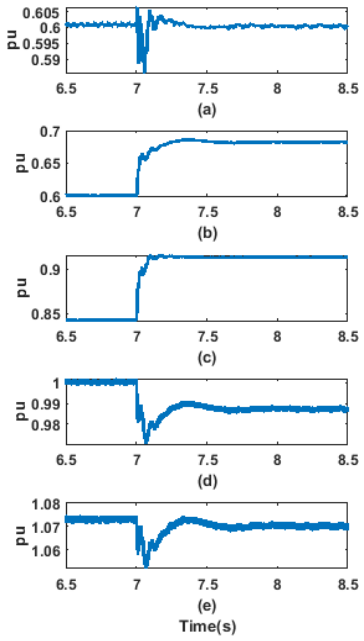

Figure 13. Constant impedance-inductive load of 0.1 pu addition. (a). Active power PCC (b). Reactive power PCC (c). Load current (d). Bus voltage (e). Machine terminal voltage

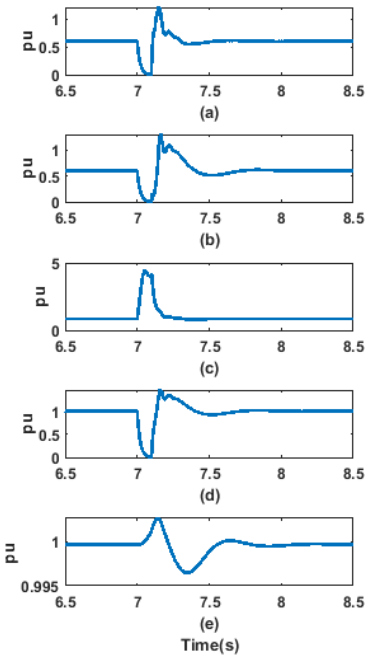

Figure 14. Three phases to ground solid fault at PCC for 0.1 s. (a). Active power PCC (b). Reactive power PCC (c). Load current (d). Bus voltage (e). Virtual rotor speed

3.4. Modified VSM0H Model.

The authors of the VSM0H model further improved its mathematical model and developed the modified VSM0H model [12]. This model also deploys decoupled control loops for P-*f* and Q-V control actions. The voltage control is achieved using conventional *v*-droop action together with a PI controller. The emulated mechanical power signal is generated using the *f*-droop action together with a PI controller. Inertial and damping responses are emulated using swing equation as the inner controller in the P-*f* controller. Modified VSM0H provides the added advantage to automatically set P and Q in grid connected mode as voltage and frequency are set by the grid. The original controller has several damping actions, current controlling, and dynamic braking, which have not been implemented in this work to enable a comparative analysis. The controller arrangement is given in Figure 15.

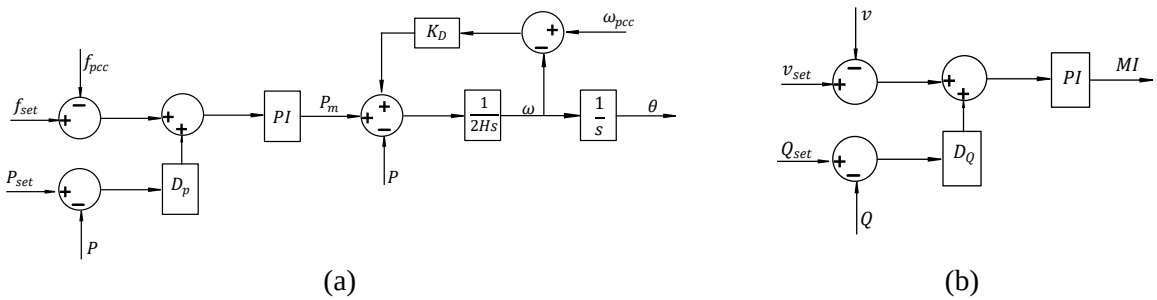

(a) (b)

Figure 15. The modified VSM0H control algorithm (a) Active Power-Frequency (P-F) controller (b) Reactive Power-Voltage (Q-V) controller

Similar to synchronverter model, this controller should have a larger time constant for the PI controller of the Q-V controller than the PI controller of the P-*f* controller. Further, depending on the H and K_D values the inner controller time constant ($2H/K_D$) will vary. Therefore, the integral time constant of the PI controller should vary in order to maintain a larger time constant for the external controller than the internal controller. The parameters are set as, P_{set} = Q_{set} = 0.6 pu, f_{set}=1 pu, v_{set}=1.2 pu, D_p = 0.03 pu, D_q= 0.03 pu, H=3 s, K_D=20 pu, proportional gain and integral time constant of P-*f* controller are K_{Pf} = 1 pu, T_{If} =0.1 s respectively proportional gain and integral time constant of Q-*V* controller are K_{Pv} = 1 pu, T_{Iv} =1.2 s respectively,. A detailed dynamic response analysis is presented next.

3.4.1. Modified VSM0H model time-domain simulation results

The dynamic responses of the system to the load adding disturbances and a solid three-phase-to-ground fault have similar patterns to the synchronverter model. The slow acting PI controller of the outer loop of the P-*f* controller has further slowed down the frequency response (Figures 16.c and 16.e). The rearrangement of the *v*-droop to regulate the voltage restores the machine terminal voltage as shown in Figure 17.e.

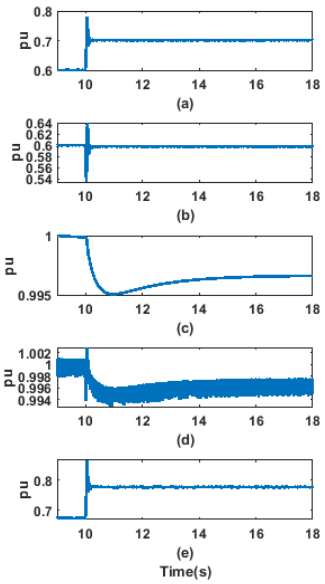

Figure 16. Constant power-resistive load of 0.1 pu addition. (a). Active power PCC (b). Reactive power PCC (c). Virtual rotor speed (d). External frequency (PLL) (e). dc power

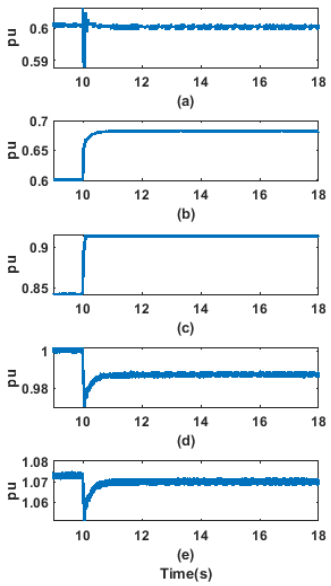

Figure 17. Constant impedance-inductive load of 0.1 pu addition. (a). Active power PCC (b). Reactive power PCC (c). Load current (d). Bus voltage (e). Machine terminal voltage

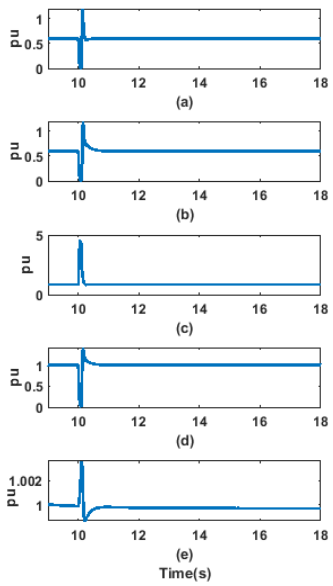

Figure 18. Three phases to ground solid fault at PCC for 0.1 s. (a). Active power PCC (b). Reactive power PCC (c). Load current (d). Bus voltage (e). Virtual rotor speed

4. CONCLUSIONS

Different inertia emulation techniques have been compared. The VSM0H model can respond spontaneously due to the absence of a slow swing control. However, it cannot support grid frequency at the initial stage of its nadir. Due to the embedded swing control, the other three controllers can smooth out the initial frequency swings. The P-*f* loop's inner controller of the modified VSM0H model can achieve a larger bandwidth by reducing virtual inertia (H) and increasing load damping (K_D). This allows the external PI controller to have a smaller time constant so that the overall response will be faster. Irrespective of the controller arrangement, the fault current for the solid three-phase-to-ground fault at the PCC caused a fault current level of around 4.5 pu. The same test system but with a similar sized hydro generator with governor, turbine, and exciter caused a 3.5 pu fault current for the same type of fault. Normally the fault current limit of the converters is less than 1.2 pu [13]. Therefore, the over-current protection of these converters is needed. The *f*-droop is a must-have feature of the VSM as it changes the power output of the converter according to the grid frequency variation and allows parallel connection of the VSMs. However, if the system operator requires inertial support as well, then the swing equation needs to be merged with *f*-droop. A larger synthetic inertia and damping means more power will be injected or absorbed for the same amount of frequency deviation. The possible inertia, damping, and steady state power sharing (*f*-droop) depend on the energy buffer available on the dc side and the converter's current rating [14]. Overall, the VSM concept allows future grids to host more converter-tied power plants without compromising power system stability.

BIBLIOGRAPHY

[1] Q.-C. Zhong, "Virtual Synchronous Machines: A unified interface for grid integration," *IEEE Power Electron. Mag.*, vol. 3, no. 4, pp. 18–27, Dec. 2016, doi: 10.1109/MPEL.2016.2614906.

[2] H. Bevrani, T. Ise, and Y. Miura, "Virtual synchronous generators: A survey and new perspectives," *Int. J. Electr. Power Energy Syst.*, vol. 54, pp. 244–254, Jan. 2014, doi: 10.1016/j.ijepes.2013.07.009.

[3] Qing-Chang Zhong, Phi-Long Nguyen, Zhenyu Ma, and Wanxing Sheng, "Self-Synchronized Synchronverters: Inverters Without a Dedicated Synchronization Unit," *IEEE Trans. Power Electron.*, vol. 29, no. 2, pp. 617–630, Feb. 2014, doi: 10.1109/TPEL.2013.2258684.

[4] S. D'Arco and J. A. Suul, "Virtual synchronous machines-Classification of implementations and analysis of equivalence to droop controllers for microgrids," in *2013 IEEE Grenoble Conference*, Grenoble, France, Jun. 2013, pp. 1–7, doi: 10.1109/PTC.2013.6652456.

[5] H. Alrajhi Alsiraji and R. El-Shatshat, "Comprehensive assessment of virtual synchronous machine based voltage source converter controllers," *IET Gener. Transm. Distrib.*, vol. 11, no. 7, pp. 1762–1769, May 2017, doi: 10.1049/iet-gtd.2016.1423.

[6] P. Kundur, *Power System Stability and Control*. New York: McGraw Hill, 1994.

[7] C. Sun, S. Q. Ali, G. Joos, and F. Bouffard, "Virtual Synchronous Machine Control for Low-Inertia Power System Considering Energy Storage Limitation," in *2019 IEEE Energy Conversion Congress and Exposition (ECCE)*, Baltimore, MD, USA, Sep. 2019, pp. 6021–6028, doi: 10.1109/ECCE.2019.8913169.

[8] J. Machowski, Z. Lubosny, J. W. Bialek, and J. R. Bumby, *Power System Dynamics Stability and Control*, Third. Wiley.

[9] M. Yu *et al.*, "Use of an inertia-less Virtual Synchronous Machine within future power networks with high penetrations of converters," in *2016 Power Systems Computation Conference (PSCC)*, Genoa, Italy, Jun. 2016, pp. 1–7, doi: 10.1109/PSCC.2016.7540926.

[10] Fang Gao and M. R. Iravani, "A Control Strategy for a Distributed Generation Unit in Grid-Connected and Autonomous Modes of Operation," *IEEE Trans. Power Deliv.*, vol. 23, no. 2, pp. 850–859, Apr. 2008, doi: 10.1109/TPWRD.2007.915950.

[11] Q.-C. Zhong and G. Weiss, "Synchronverters: Inverters That Mimic Synchronous Generators," *IEEE Trans. Ind. Electron.*, vol. 58, no. 4, pp. 1259–1267, Apr. 2011, doi: 10.1109/TIE.2010.2048839.

[12] A. J. Roscoe *et al.*, "A VSM (virtual synchronous machine) convertor control model suitable for RMS studies for resolving system operator/owner challenges," 2016.

[13] N. Baeckeland, B. Herteleer, and M. Kleemann, "Modelling fault behaviour of power electronic converters," *Int. J. Electr. Power Energy Syst.*, vol. 123, p. 106230, Dec. 2020, doi: 10.1016/j.ijepes.2020.106230.

[14] S. D'Arco, J. A. Suul, and O. B. Fosso, "A Virtual Synchronous Machine implementation for distributed control of power converters in Smart Grids," *Electr. Power Syst. Res.*, vol. 122, pp. 180–197, May 2015, doi: 10.1016/j.epsr.2015.01.001.